Modelling alpine permafrost distribution in the Hohe Tauern region, Austria

Lothar SCHROTT[1)*)], Jan-Christoph OTTO[1)], Felix KELLER[2)]

[1)] Department of Geography and Geology, University of Salzburg, Salzburg, Austria;

[2)] Academia Engiadina, Samedan, Schwitzerland;

[*)] Corresponding author, lothar.schrott@sbg.ac.at

Abstract

Knowledge concerning permafrost distribution in the Alps is an important prerequisite to estimate potential developments caused by climate change. An assessment of natural hazards or the creation of risk maps in high alpine catchments very often requires the consideration of potential permafrost occurrence. The present study for the first time shows a high resolution and index based permafrost distribution for the region Hohe Tauern (approx. 4400 km²), which is based on the empirical model PERMAKART 3.0. The approach integrates three different relief classes (rock walls, steep slopes, foot slope position) in a topoclimatic key. The used thresholds were calibrated with field observations (geophysical soundings, mapping) and adjusted to our study site. The modelling results were validated with more than 600 BTS (bottom temperature of snow cover) measurements. At present an area of 550 km² is affected by permafrost to a lesser or greater extent. The occurrence of permafrost varies according to aspect and relief conditions in some locations more than 1000 m in altitude. Low altitude sporadic permafrost occurrence is possible in shady northerly exposed slopes at 2000 m a.s.l., whereas southerly exposed rock walls remain permafrost free even above 3000 m a.s.l. In the national park "Hohe Tauern" (1856 km²) 25% of the area is underlain by permafrost. A simple scenario taking into account a possible temperature increase of 1 K would lead to widespread permafrost degradation. The produced permafrost map assists planers and decision-makers and contributes to better understanding of our mountain ecosystem.

Die Kenntnis der Permafrostverbreitung in den Alpen ist eine wichtige Voraussetzung zur Abschätzung möglicher Veränderungen durch den Klimawandel. In hochalpinen Einzugsgebieten erfordert die Abschätzung von Naturgefahren oder die Erstellung von Gefahrenhinweiskarten den Einbezug potentieller Permafrostgebiete. Die vorliegende Studie zeigt erstmals für die Hohen Tauern (rund 4400 km²) eine hochaufgelöste indexierte Permafrostmodellierung, die mit dem empirischen Modell PERMAKART 3.0 unter Berücksichtigung von drei Reliefklassen (Felsflächen, Steilhang, Hangfußlagen) in einem topo-klimatischen Schlüssel umgesetzt wurde. Die dafür verwendeten Grenzwerte wurden mittels Geländebefunden (u.a. geophysikalische Untersuchungen, Kartierungen) an das Untersuchungsgebiet angepasst. Die Modellergebnisse sind mit über 600 BTS (Basistemperatur der winterlichen Schneedecke) Messungen aus sechs Testgebieten validiert worden. Gegenwärtig ist auf einer Fläche von 550 km² mit dem Auftreten von Permafrost zu rechnen, wobei je nach Exposition und Reliefbeschaffenheit das mögliche Auftreten von Permafrost um über 1000 Höhenmeter variieren kann. Vereinzelt tritt Permafrost in strahlungsarmen Nordexpositionen schon in Höhenlagen um 2000 m auf, dagegen ist in steilen südexponierten Felslagen erst oberhalb von 3000 m diskontinuierlicher Permafrost anzutreffen. Im National-park "Hohe Tauern" (1856 km²) unterliegt rund 25% dem Einfluss von Permafrost. Ein einfaches Szenario unter Verwendung eines möglichen Temperaturanstiegs um 1 K deutet auf eine großflächige Permafrostdegradation hin. Die Permafrostkarte liefert Umweltplanern und Entscheidungsträgern wertvolle Hinweise zur regionalen Permafrostverbreitung und trägt zu einem besseren Verständnis unseres Gebirgsökosystems bei.

1. Introduction

Detailed knowledge about the current permafrost occurrence is of crucial importance with respect to climate change. In mountain areas, however, permafrost distribution is spatially very heterogeneous and available models have several limitations and uncertainties. Moreover, permafrost is a thermal phenomenon, defined by temperatures of lithosphere material at or below 0°C during two or more consecutive years, and sensitively reacts to increasing temperatures but is not easy to detect (Harris et al., 2003; Noetzli et al., 2007; Noetzli and Gruber, 2009; Haeberli et al., 2010). Thawing permafrost is one consequence of warming trends in the European Alps which causes a continuous change in permafrost distribution and

influences a number of earth surface processes such as rock falls or debris flows (Krainer, 2007; Sattler et al., 2011; Deline et al., 2012). In this context, the International Permafrost Association in most recent resolutions (www.permafrost.org) has recommended that new innovative and accurate maps of permafrost for use by multiple audiences and outreach products regarding permafrost should be developed.

Systematic scientific investigations concerning mountain permafrost in the European Alps started in the early 1970s although the first paper describing a rock glacier in the Austrian Alps dates back to the 1920s (Finsterwalder, 1928). Pioneering work on mountain permafrost was mainly focused on rock

glaciers and rules of thumb for alpine permafrost occurrence were established in 1975 (Barsch, 1973; Haeberli, 1975).

Later on in 1992 these rules of thumb related to alpine permafrost distribution, were transferred into a digital ArcInfo platform considering parameters such as altitude, aspect and snow avalanche deposits (Keller, 1992). This date can be considered as the birthday of the first digital permafrost distribution map for a part of eastern Switzerland by using an empirical model which relates permafrost occurrence to the topoclimatic factors elevation, slope, aspect, air temperature and solar radiation. First digital permafrost distribution models, such as PERMAKART or PermaMap, were developed for parts of Switzerland using empirical-statistical approaches and DEMs (Keller, 1992; Hoelzle, 1992).

In Austria permafrost research similarly to Switzerland has a long tradition but for decades the focus was on rock glacier distribution and dynamics mostly on local scale (e.g. Patzelt and Haeberli, 1982; Lieb, 1996; Kellerer-Pirklbauer, 2005; Krainer, 2007). The first empirically validated Swiss permafrost map was published in 1998 (Keller et al., 1998). Early attempts regarding permafrost distribution in the Austrian Alps were based on an extensive rock glacier inventory of the Eastern Austrian Alps (Lieb, 1996, 1998). For the entire Austrian Alps a first digital permafrost distribution map with an adapted topoclimatic key was created by Ebohon and Schrott (2008). The model used herein integrates ideas which were established in the classic PERMAKART and PERM models (Keller, 1992; Imhof, 1996).

Austria has currently a surface area of approximately 1600 km² which is underlain by permafrost (Ebohon & Schrott, 2008). Although this constitutes to only 2% of its entire territory, in its western part, like Tyrol, it can be as much as 10% and in the Hohe Tauern mountain region we expect extensive permafrost above 2500 m a.s.l. exceeding the surface area of present glaciers.

The most recent development concerning permafrost zonation for the European Alps is related to the PermaNet initiative, which produced a permafrost map for the entire European Alps based on the explanatory variables mean annual air temperatures, potential solar radiation and mean annual precipitation (Cremonese et al., 2011; Mair et al., 2011). We will discuss one of the outcomes of this project with our modelling results presented in this paper. A global permafrost model derived from an approach using mean annual air temperature for the reference period 1961-1990 was recently published by Gruber (2012). The resolution and aim of such a global approach is, however, incomparable with the present study. Nevertheless this study provides valuable estimates on a global scale and lists permafrost extension for the top 25 countries with permafrost occurrence (Gruber, 2012).

Modelling the occurrence and distribution of mountain permafrost using either empirical, empirical-statistical or process-physically based models has been applied also elsewhere in Europe, North America or Asia (e.g. Etzelmüller et al., 1998, Tanarro et al., 2001; Isaksen et al. 2002; Heggem et al. 2005;

Ridefelt et al. 2008; Lewkowicz and Bonnaventure, 2008; Bonnaventure et al., 2012; Lewkowicz et al., 2012; Janke et al., 2011; Li et al., 2008).

The main objectives of this study are to

(i)   develop a new index-based accurate permafrost distribution map for a mountain area in the Austrian Alps (Hohe Tauern),

(ii) to calibrate and validate the empirical approach with numerous field evidences (bottom temperature of snow cover, field geophysics, geomorphological mapping), and

(iii) to assist the national park administration "Hohe Tauern" with a valuable outreach product for science and education purposes.

Scenarios about the future development of permafrost extension are not reliable without accurate estimates of both spatial extent and thermal conditions. Thus, knowledge concerning permafrost distribution is of crucial importance to assess permafrost related slope instabilities and rock fall hazards (Fig. 1).
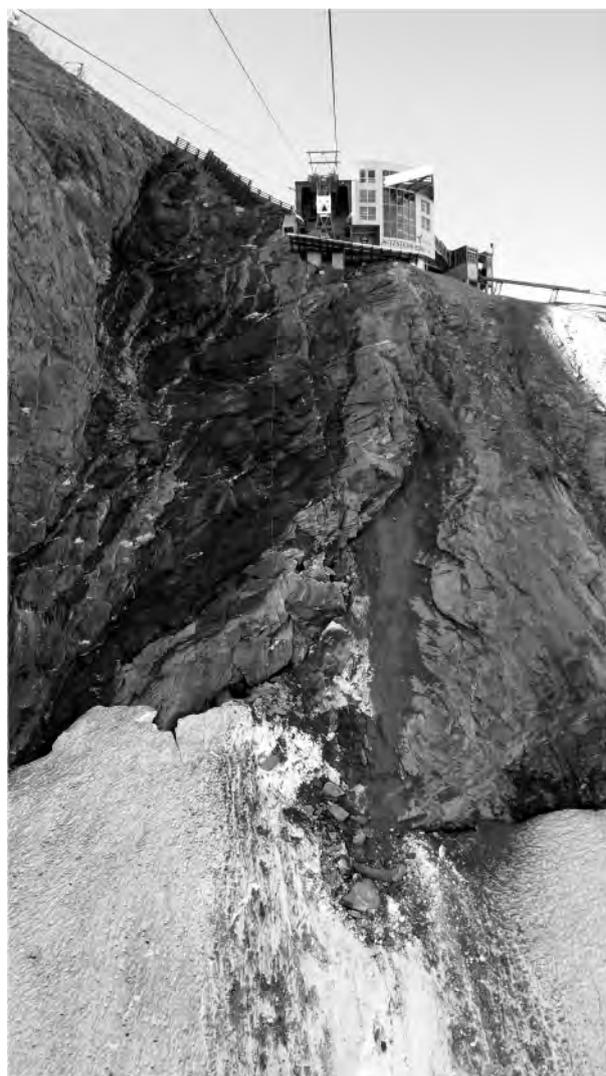

FIGURE 1: Permafrost related rock fall at the Kitzsteinhorn at approx. 2950 m (August 18, 2012 at 3pm). At the slip surface ice became visible after the failure. The Kitzsteinhorn region is one of our six test sites (see Fig. 2)

The outcome of this study contributes to a better understanding of current permafrost distribution.

2. Study area

The study area Hohe Tauern in Austria is situated in Salzburg, Eastern Tyrol and Carinthia, which form part of the eastern European Alps (Fig. 2). The area under investigation comprises the "Hohe Tauern" national park (1856 km²) and ist surroundings with a total surface area of approximately 4400 km² (Table 1). The mountain ranges of Venedigergruppe, Granatspitzgruppe, Glocknergruppe, Schobergruppe, Goldberggruppe und Ankogelgruppe all belong to this area and comprise partly glacierized catchments. Within the Großglockner massiv (3798 m), representing the highest mountain peak of the Austrian Alps, the longest glacier Pasterze (8.4 km) is located (see Fig. 3). With the exception of the Großglockner massiv the currently glacierized areas decrease from west to east following lesser elevations. A lithological characteristic of the area is the Tauern window with predominantly high grade metamorphic rocks.

The steep relief, low MAAT (mean annual air temperature), intensive weathering (frost shattering) and sufficient debris supply favours the development of rock glaciers in cirques, a predominant landform in the eastern part of the Hohe Tauern, and of the Schobergruppe in particular. Numerous active rock glaciers in the Hohe Tauern region indicate the presence of discontinuous permafrost (Barsch, 1996; Krainer and Mostler, 2002). The climate is more humid in the north-west and becomes more continental in the southern and eastern parts. Within our study area we have selected six test sites for extensive local permafrost investigations, ground truth observations and validation purposes. Namely, from west to east: the Obersulzbachtal (glacierized), the Amertal, the Kitzsteinhorn (glacierized), the Glorer Huette, the Gradental, and the Kreuzkogel (see Fig. 2).

3. Methods and data

In the field we applied measurements of the bottom temperature of snow cover, ground surface temperature recordings using UTL logger, and field geophysics (DC-resistivity, ground penetrating radar) (Table 2). In addition we carried out geomorphological mapping of rock glaciers. This information was used to calibrate the topoclimatic key.

3.1 Bottom-temperature of snow cover (BTS) and ground surface temperature (GST)

The bottom temperature of snow cover was introduced by Haeberli (1973) and is defined as the temperature measured at the snow/ground interface at the end of the winter (typically between February/March and April). A sufficient insulation against solar radiation and air temperature is provided by a snow depth of 80 to 100 cm. In our study we used the follo-
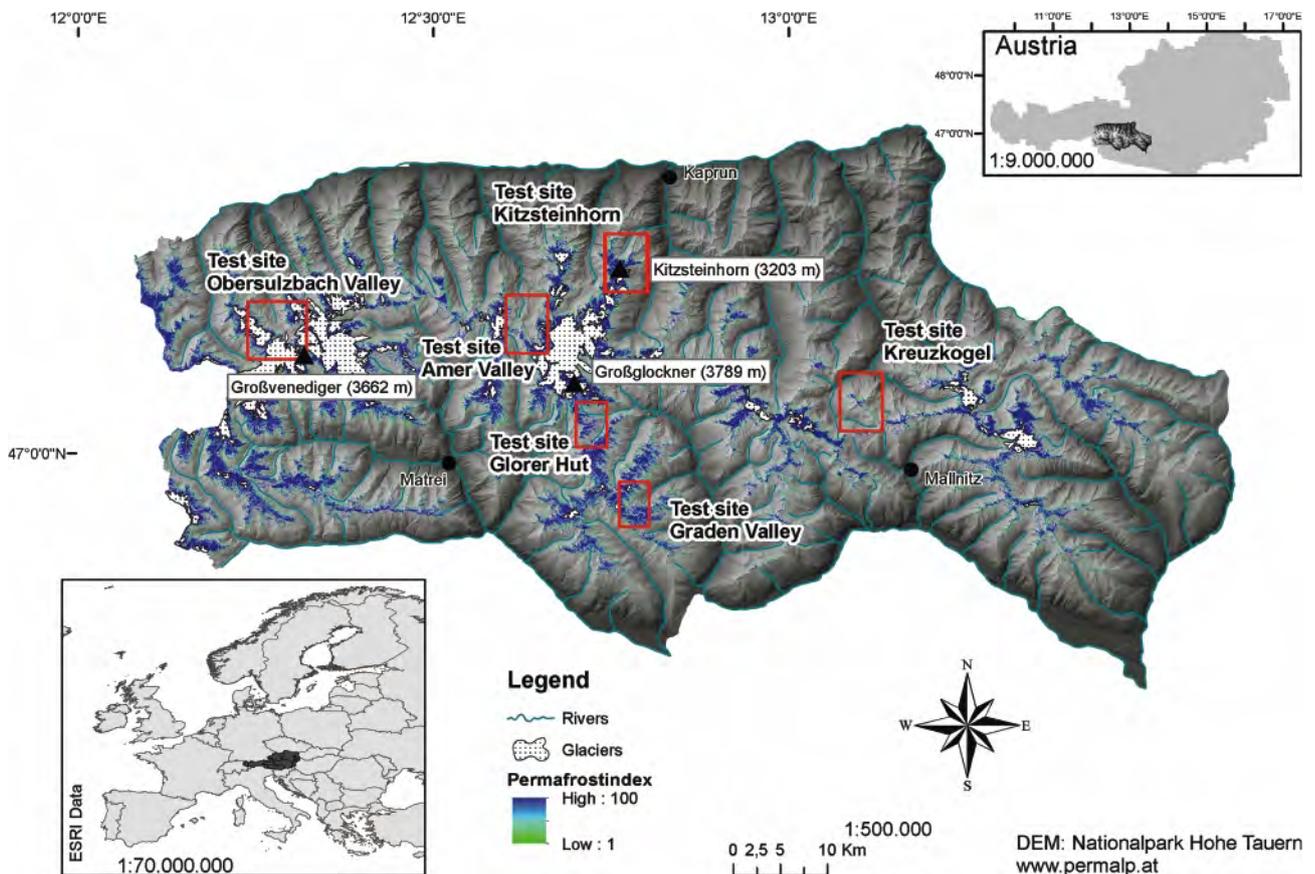

Figure 2: Permafrost distribution map of the "Hohe Tauern" region and location of six test sites. Extensive field work was carried out for local permafrost detection and validation purposes (central Austrian Alps). Please note: the map can be downloaded at www.permalp.at/downloads-html.

wing classical thresholds as permafrost indicators:

>2°C: permafrost unlikely

2-3°C: permafrost possible, uncertainty range

<3°C: permafrost probable.

In total we carried out 626 BTS measurements within our six test sites in order to obtain a reasonable amount of data for the model validation. Usually we used carbon fibre avalanche sticks equipped with PT 100 (0.1°C accuracy). During measurement we paid attention to measure through a homogenous snow pack (avoiding icy freezing levels) and we tried to make sure that the stick touched the ground. The sampling strategy was to measure grid based or along transects with intervals between 5 and 20 m. In addition we installed at different locations 25 Universal Temperature Loggers (UTL) to record ground surface temperature (GST). The UTL-1 and UTL-3 loggers (Universal Temperature Logger, Geotest) are provided with an accuracy of +/-0.1 °C. With these loggers we recorded temperature variations throughout the year at the surface (depth approx. 1cm). Winter temperature can be also a useful indicator of permafrost absence or presence. A very typical temperature course throughout the year in one of our test sites with permafrost occurrence is shown in Figure 4.

3.2 Field geophysics

Electrical resistivity (ERT) and ground penetrating radar (GPR) are meanwhile standard tools for permafrost detection (Hauck and Kneisel, 2008; Schrott and Sass, 2008). In order to compensate uncertainties when using only one indirect prospection technique, the application of additional geophysical methods is highly recommended (Otto and Sass, 2006; Schrott and Sass, 2008). Both methods provide reliable and often very precise information of frozen or unfrozen subsurface debris or rock in mountainous regions. In this study we used our results of geophysics to calibrate the topoclimatic key and to cross check with BTS and modelling results (see Otto et al., 2012;

Figure 3: Großglockner with the lower tongue of Pasterze glacier (view to NW). On the north-east facing slopes (upper left) widespread permafrost can be expected. (Foto: August 2009, L. Schrott)

Otto et al., 2011).

High contrasts in electrical resistivity between frozen and unfrozen debris and rock facilitate the identification of permafrost occurrence. Consequently, subsurface resistivity was recorded at 25 different locations in our test sites using a Geo-Tom MK8E1000 multi-electrode resistivity system with multiple electrodes and electrode spacing between 1 and 4 m. ERT was analysed with the Res2DInv software package. Different measurement times, however, inhibited an exact overlap of the GPR and ERT profiles.

A total of 12 GPR profiles were measured with lengths between 60 and 140 m. We used a MALA RAMAC system with 100 and 250 MHz shielded and unshielded antenna system. The measurement was usually applied with a station spacing of 5 cm triggered by a string and using a sample frequency of 2553 MHz. Within a time window of 204 ns a total of 32 stacks were obtained. This configuration results in a vertical resolution of about 20 cm and a lateral resolution of about 50 cm
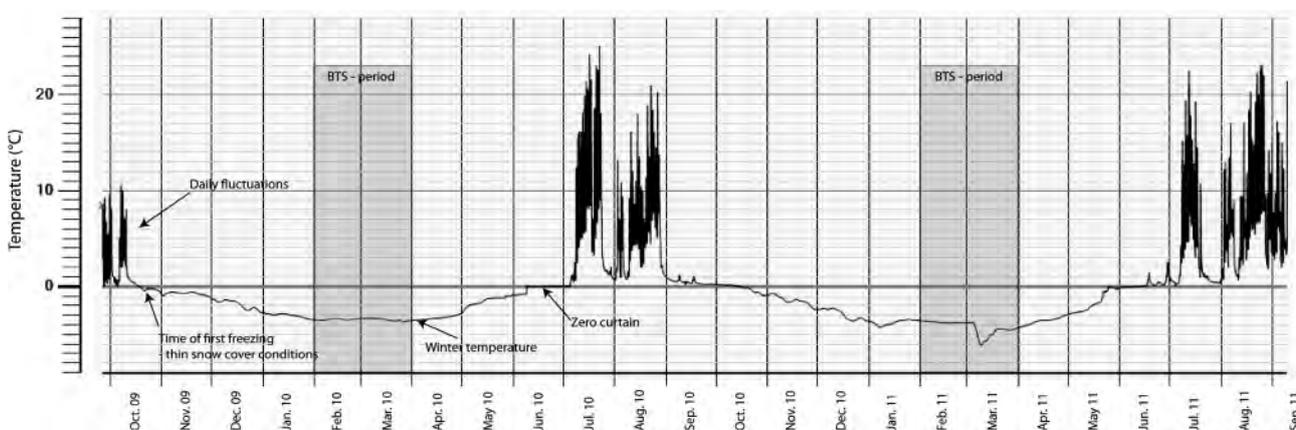

Figure 4: Typical annual temperature course of a recorded ground surface temperature (GST) at a permafrost site using our universal temperature loggers. Location is at 2890 m a.s.l. at Maurerkogel, Kitzsteinhorn. (a) High diurnal variations during the snow free period from late spring to fall are caused by high air temperature variations; (b) in late fall and early winter GST shows pronounced negative values due to thin or missing snow cover; (c) during wintertime and with sufficient snow cover which provides isolation from atmospheric influences fluctuation of temperature is damped to a minimum, the winter temperature is reached with heat flux coming from the subsurface. This is the typical time period for bottom temperature of snow cover measurements (BTS); (e) the GST temperature increases again in spring due to thin or missing snow cover but remains constant at 0°C over several days because the phase transition of ice to water is retarded by latent heat absorption ("zero curtain").
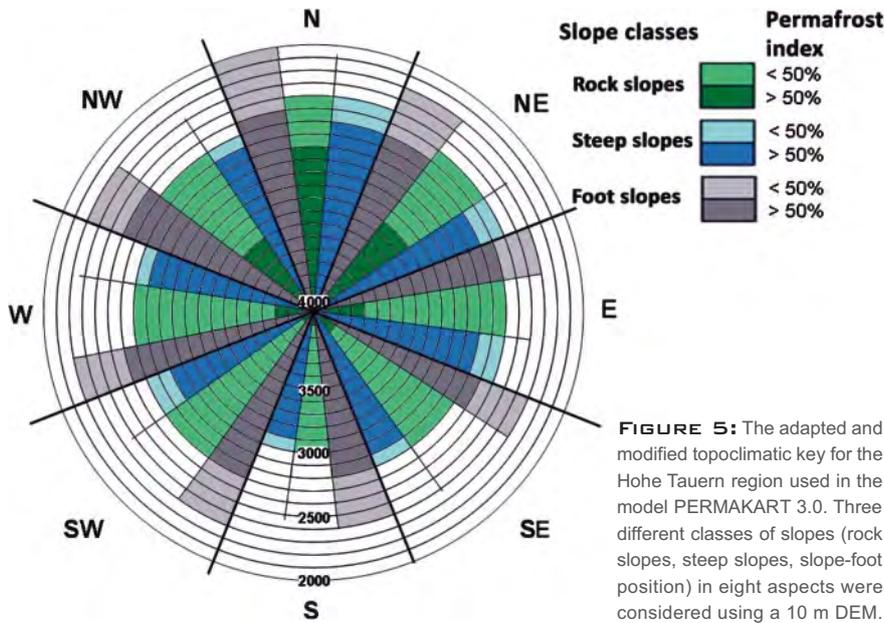
Figure 5: The adapted and modified topoclimatic key for the Hohe Tauern region used in the model PERMAKART 3.0. Three different classes of slopes (rock slopes, steep slopes, slope-foot position) in eight aspects were considered using a 10 m DEM.

tion can be considered indirectly by means of a topoclimatic key which distinguishes between slope and foot of slope locations (Haeberli, 1975). In our study we used a new topoclimatic key which represents - beside different altitudes and aspects - three classes of relief (Fig.5). The topoclimatic key contains 24 different "relief classes" subdivided in eight different aspects each with three slope angles classified as rock slopes/walls, steep slopes (>11°) and slope foot-positions. The relief parameters altitude, slope angle and aspect can be regarded as representations of climatic variations influencing the permafrost distribution. The altitudinal limits were adjusted to the Eastern Austrian Alps and differ from the original topoclimatic key which was developed for Switzerland in the model PERMAKART 1.0 (Keller, 1992; Ebohon and Schrott, 2008). PERMAKART uses the statistical relationship between topographic parameters and empirically identified permafrost occurrences. For the model validation we used our BTS and GST measurements. Model calibration was realised in an iterative process using field data from geophysics which indicate permafrost absence or presence. These data were subsequently used for a further adjustment of the altitudinal limits with a general upwards shift of 50 m compared to the previous topoclimatic key applied by Ebohon and Schrott (2008). These previously used lower limits of permafrost were mainly based on intact rock glacier occurrence.

(for permafrost environment, v ~ 0.13 m ns-1 at one meter depth) (Trabant, 1988). GPR raw data was analysed using REFLEXW software applying standard filter routines; in addition migration and topographic correction was applied. The data interpretation is based on the propagation velocity of the radar waves and the velocity measurements are obtained by hyperbola analyses. Winter conditions, subsequent snow cover and low subsurface water content, facilitated the application of GPR and improved the data quality. The measurements generated high-resolution, low noise data that also contain the snow depth and the accurate position of the slope topography.

3.3 Empirical-statistical GIS modelling

Permafrost occurrence is influenced by climatic (air temperature, solar radiation), topographic (aspect, slope), and site specific surface conditions (snow cover and duration, debris and boulder size). Air temperature and potential solar radia-

The empirical model PERMAKART 3.0 used herein is a consequent development of the classic PERMAKART model with several new components. An innovative amelioration is the index-based classification of permafrost probability from 1 to 100.

To calculate the permafrost index, all possible slope expositions and the flat areas were considered. The variables h1 and h2 considered for slopes whose inclination is above 11° and slope bottoms describe the lower limits of the elevation zone with possible (h1) and probable (h2) permafrost existence after Haeberli (Haeberli, 1975). At the elevation of the lower limit with possible permafrost existence (h1) the permafrost index is set to 1. At the elevation of the lower limit with probable permafrost (h2) existence the permafrost index is set to 50. Between h1 and h2 the permafrost index is related to increasing elevation in a linear way. Above h2 the permafrost index is calculated using the formula: y = 50 + (x - h2) * 0.1 until it reaches 100 (Fig. 6).

In the rock areas slope inclination is also considered as a factor. H2 is corrected with a value (y) in relation with the inclination (x) as follows: $y = 0.1875x2 - 36.25x + 1500$ (40° < x < 80°). In steep areas the permafrost limit lies generally higher, i.e. with altitude correction, the permafrost index for

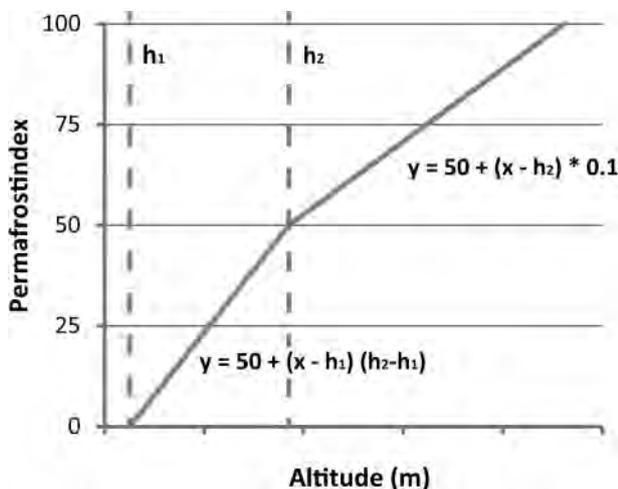**Figure 6:** Calculation of the permafrost index using the new topoclimatic key (see Fig. 5).

slope inclinations < 60° increases, while in steep situations > 60° it decreases.

This allows a more transient and realistic visualisation avoiding sharp boundaries. It replaces the previous two classes with possible and probable permafrost distribution. The previous boundary between possible and probable permafrost receives an index of 50. All areas above this limit receive an index-based increase of ten points per 100 m. This approach was originally developed within the Swiss national Program 31 and was applied in a glaciological map of the Engadin, Switzerland (Keller et al., 1998). A further important improvement of PERMAKART 3.0 is based on the new findings regarding rock permafrost temperatures (Gruber et al., 2004). Rock walls between 50° and 70° steep show significantly higher temperatures which may lead up to several hundred meters higher elevations of lower limits of permafrost. In contrast, very steep rock faces with inclinations over 70° become colder again. These findings were included in our model by modifying the DEM with correction shifts of lower permafrost limits up- and downwards, respectively.

In addition to steep slopes and foot-slope positions we therefore added in the new model rock slopes as a separate unit which considers somewhat higher altitudinal limits compared to steep slopes (Fig. 5). All areas above 45° were modelled as rock slopes. To improve spatial accuracy we used a DEM with a grid resolution of 10 m.

4. Results

For the entire study area of the Hohe Tauern region (4378 km²) we estimate with our model an area of 550 km² which is currently underlain by permafrost to a lesser or greater extent. This corresponds to approximately 13% of the total area. For the national park "Hohe Tauern" with a surface area of 1856 km² the permafrost area becomes even more predominant with almost 25% (Table 1). More than 40% of the permafrost area shows index values higher than 50. In comparison to permafrost, glaciers cover only 160 km² showing currently a strong retreat which leads to a decrease in both surface area and ice volume. At high altitudes and favourable (cold) conditions this may even lead to permafrost aggradation in glacier forefields (Kneisel and Kääb, 2007). At present we ob-

Total area (4379 km²)	Permafrost distribution (km²)	Portion of surface area underlain by permafrost (%)	Glacier surface area (2003)
Study area	553.2	12.6	163.2
State Salzburg	182.8	2.6	60.8
State Tyrol[1]	218.4	10.8	66.2
State Carinthia	152	1.6	36.2
National park[2] "Hohe Tauern" (1856 km²)	455.4	24.5	159.8

[1] only East Tyrol; [2] includes states of Salzburg, East Tyrol and Carinthia

TABLE 1: Surface areas underlain by permafrost and glaciers for the national Park "Hohe Tauern" and the states of Salzburg, East Tyrol and Carinthia.

Method	Total number of measurements	With indication of permafrost occurrence
BTS	626	332
GST (UTL)	25	12
DC-resistivity (ERT)	25	12
GPR	12	5

TABLE 2: Field measurements for permafrost detection in our six test sites.

serve especially between 3000 and 3500 m a.s.l. the most extensive glaciation. As a consequence, this altitudinal belt is characterized by a lesser permafrost extension (see Fig. 7). The total permafrost extension for all subareas of the region is summarized in Table 1.

A comparison with the previous model used by Ebohon and Schrott (2008) shows a significant improvement. The new mo-del is based on a better resolution (10 m instead of 50 m) and shows - due to the index-based visualization and the additional rock class - a more realistic pattern of the permafrost ex-
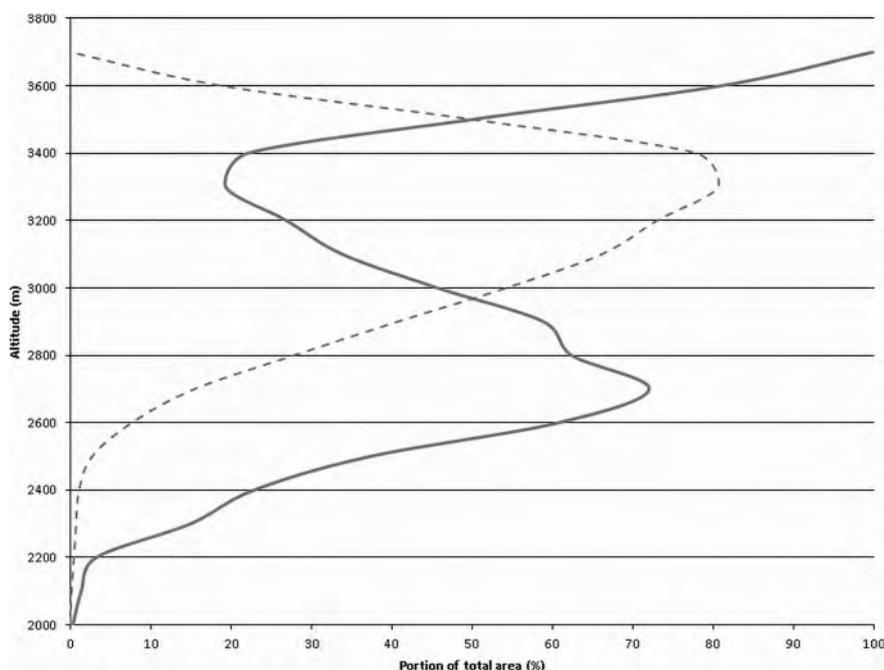

FIGURE 7: Hypsometrical curves of glacier (- - -) and permafrost extension (——) derived from our data set used in the PERMAKART 3.0 model.
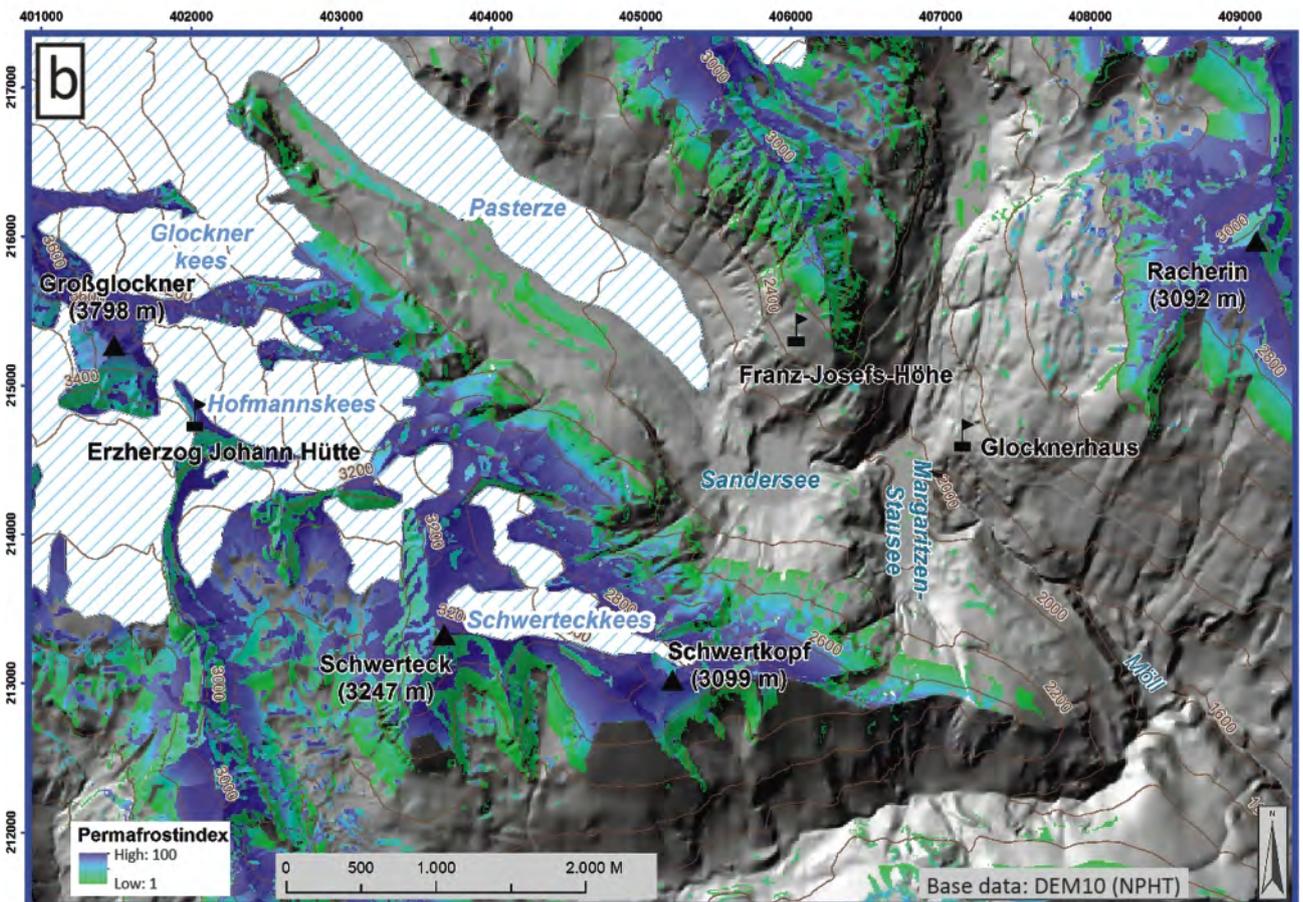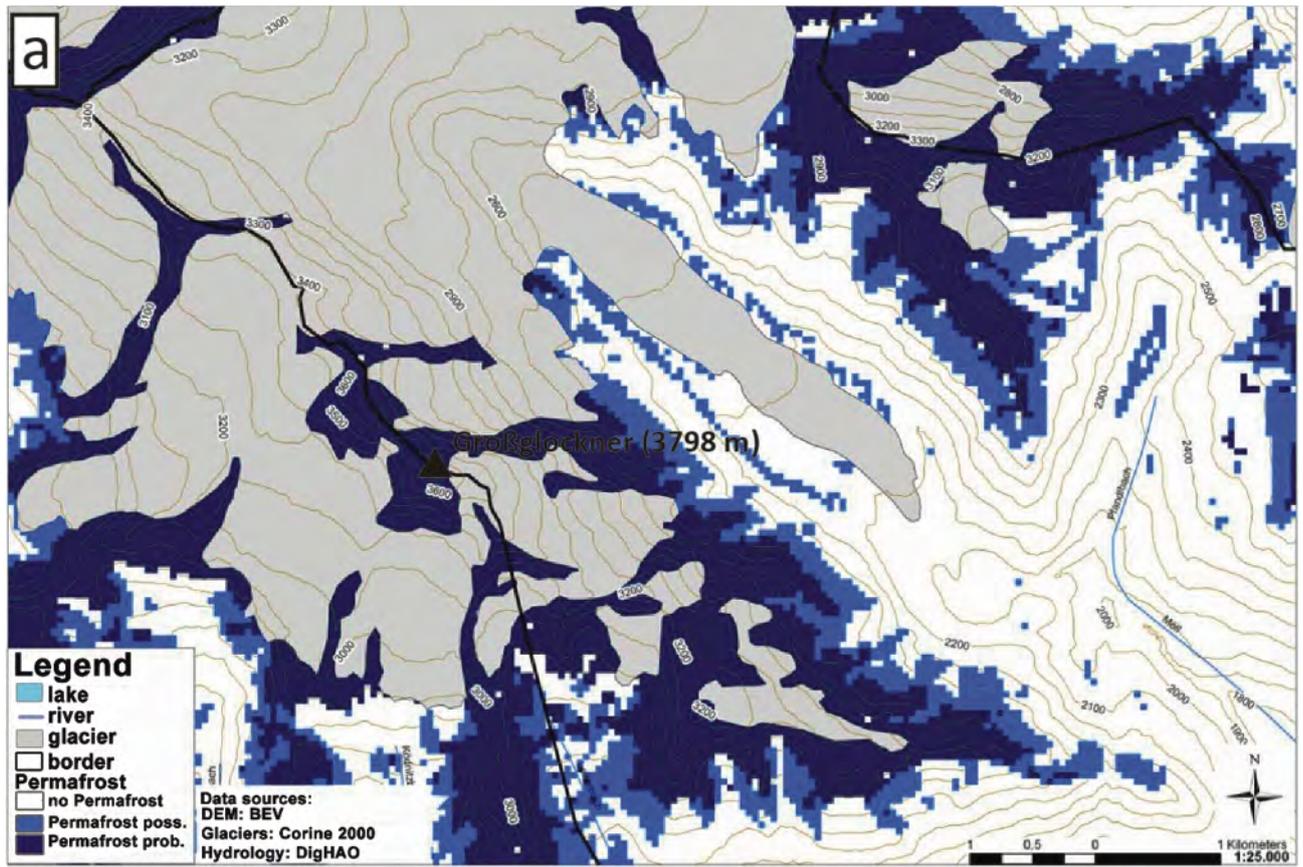
FIGURE 8: Comparison of the permafrost distribution in the Großglockner/Pasterze region. (a) simulation with the previous model used by Ebohon and Schrott (2008) based on a 50 m DEM. (b) simulation with the new PERMAKART 3.0 used in this paper based on a 10 m DEM and considering rock slopes in a separate relief class.
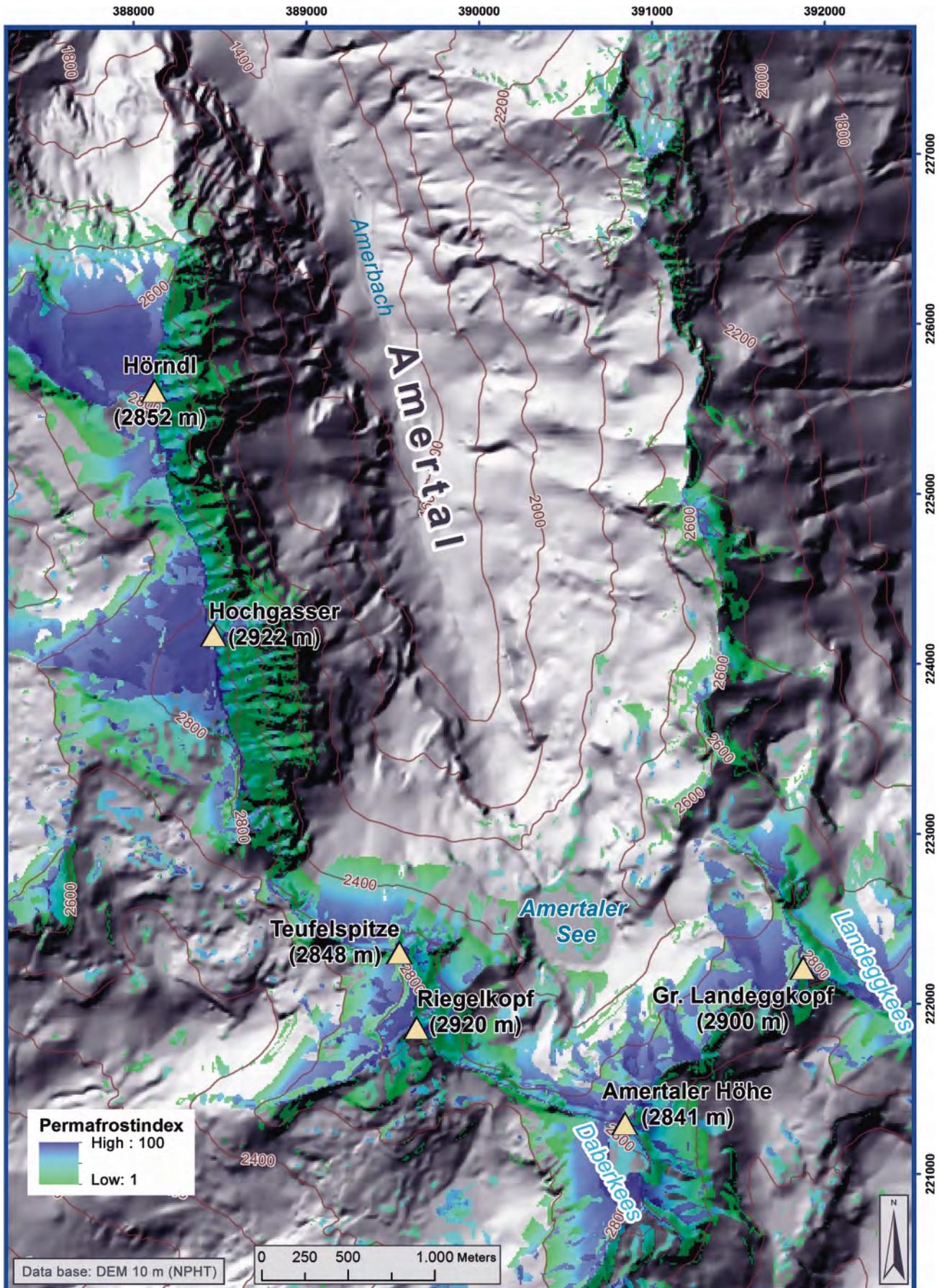
FIGURE 9: Modelled permafrost distribution in the Amertal. Pronounced differences of permafrost probability are visible at the left between the peaks Hörndl and Hochgasser. Northeast facing slopes are steep rock faces whereas west facing slopes are debris slopes leading to higher permafrost probabilities even in lower altitudes.
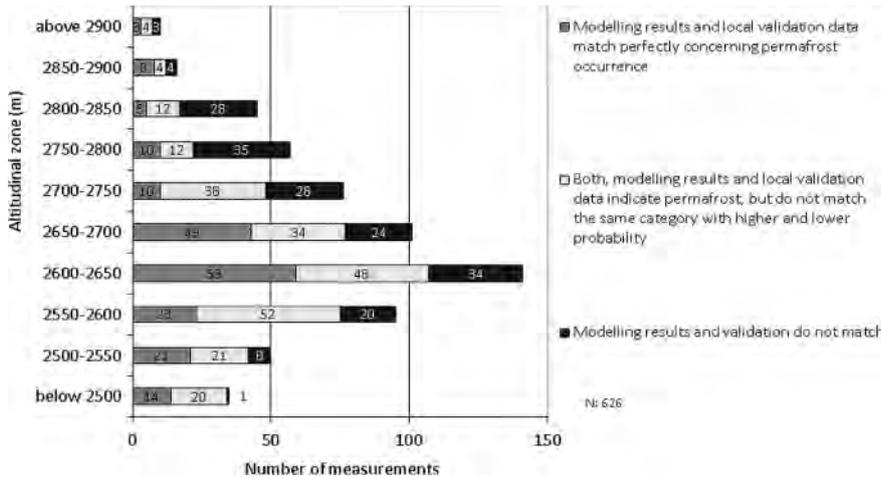
FIGURE 10: Comparison of modelling results with obtained BTS values classified in altitudinal belts between 2500 and 2900 m and below 2500 and above 2900 m a.s.l., respectively.

tension according to topographic heterogeneities (Figs.7 and 8). In areas with contrasting rock and debris surfaces in close proximity to each other the effect of the new integrated rock class becomes very effective within the applied topoclimatic key (Fig. 9).

The topoclimatic key for the Hohe Tauern displays threshold values (m a.s.l.) for permafrost occurrence. According to this approach permafrost can occur on north facing steep slopes

(between 11 and 45 degrees) above an altitude of 2400 m, whereas on south facing slopes higher permafrost indices can be only expected above 3000 m (Fig. 5). In slope foot-positions permafrost probability is modelled down to 2000 m a.s.l. on north facing slopes compared to 2400 m at south facing slopes. We know, however, that some isolated permafrost patches occur even in lower altitudes, but this cannot be displayed with the model used.

4.1 FIELD GEOPHYSICS

The Amertal was one of our key test sites and the modelling result shows how different permafrost occurrence is displayed in topographic heterogeneous terrain (Fig. 9). Figure 9 also shows the patchy permafrost occurrence around the lake according to our model. This result fits well with our findings using electrical resistivity tomography (ERT) and ground penetrating radar (GPR) (Otto et al., 2011). ERT and GPR soundings are found to be very useful for local permafrost detection and subsurface structures (Hauck and Kneissl, 2008; Schrott and Sass, 2008). Generally, we interpret resistivity values > 10,000 Ω m as ground ice or permafrost occurrence which is in accordance with previous studies (Hauck and Kneisel, 2008). Localities showing resistivities below 10,000 Ω m can be regarded as non-frozen regolith. Strong reflection patterns and propagation velocities between 0.13 and 0.16 m ns-1 in the radargrams indicate ground ice or permafrost (Berthling and Melvold, 2008). For details regarding local permafrost detection using geophysics in our test sites we refer to Otto et al. (2012), Otto et al. (2009) and Keuschnig et al. (2012).

4.2 VALIDATION OF MODELLING RESULTS

BTS values provide the most comprehensive data set with a total of 626 measurements and allow a sophisticated validation in all six test sites. Local permafrost detection by BTS measurements was, however, in some cases problematic due to variable subsurface conditions and internal structure of snow cover. The validation result is classified in three categories.

(a) modelling results and local validation data match perfectly concerning permafrost occurrence;

(b) both, modelling results and validation data indicate permafrost, but do not match the same category with higher and lower probability;

(c) modelling results and validation data do not match.

Most data were collected in the sensitive zone between 2500 and 2900 m a.s.l. with mostly sporadic or discontinuous permafrost probability (see Fig. 10). Permafrost occurrence is matched by overall 69%, classified into 46% in category (a) and 23% in (b), respectively (Fig. 10). Very good matching is achieved in southeast, south and southwest-facing slopes.
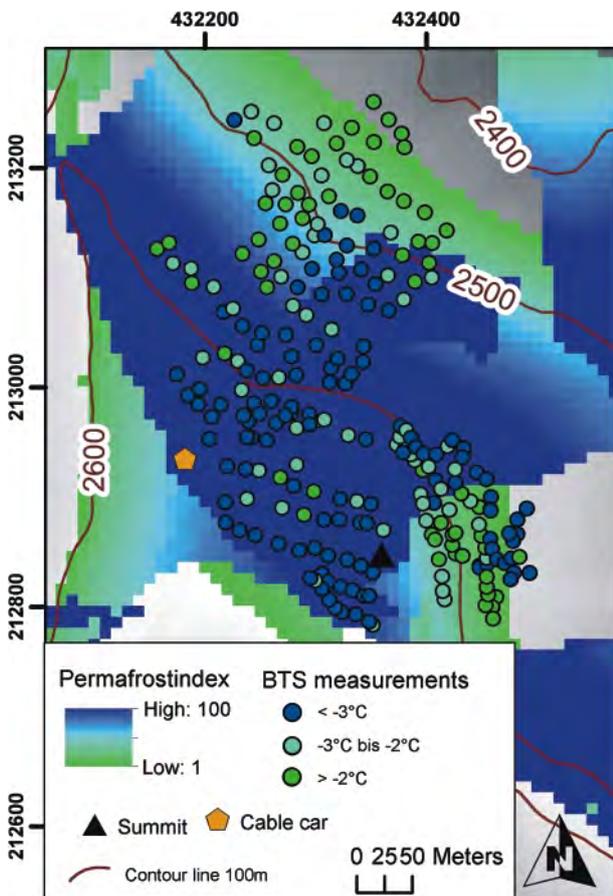

FIGURE 11: Detailed permafrost probability map of our test site Kreuzkogel and BTS data.

Larger discrepancies can be observed in north, northeast and east-facing slopes. Slope aspect, however, cannot explain the variance of the data quality, because this effect is mainly influenced by the variable snow cover and by subsurface condition.

5. Discussion

The visualized permafrost distribution in the Hohe Tauern region primarily serves as an indication map at a regional scale. It assists planers in permafrost related constructions but does not substitute local investigations if detailed knowledge concerning permafrost occurrence is required. The map provides valuable input data for permafrost scenarios and contributes to a better understanding of our geosystem.

Explanations concerning mismatches of BTS data and modelling results can be the result of one or more of the following circumstances:

(i) point measurement versus raster data (resolution problem),

(ii) water or icy layers within the snow cover,

(iii) insufficient insolation of the snow cover (duration too short), and

(iv) limited validity of the BTS thresholds due to heterogeneous and coarse blocky subsurface.

The latter three conditions can significantly influence the BTS temperature and hence the effectiveness of the method using the classical thresholds (< -3°C permafrost probable; > -2°C permafrost unlikely; between -2 and -3°C permafrost possible, uncertainty range). A comparison of our modelling results with geophysical data shows that BTS is not always the ideal proof concerning permafrost occurrence. In one of our test sites we made an extensive small scale investigation using DC-resistivity, GPR sounding and BTS measurements (Otto et al., 2012). A comparison between field geophysics and BTS data explains to some extent mismatches with our modelling results. In this context, Otto et al. (2012) pointed out that small scale variations of the surface by boulders can significantly influence the permafrost condition. The authors showed that surface roughness and solar radiation varies almost diametrically opposed indicating the effect of large boulders on the energy input. The influence of shading effects in mountain regions

is well known and can have significant impact on local permafrost occurrence (Schrott, 1994; Schrott, 1996). In coarse and blocky terrain subsurface ventilation can locally reduce ground temperature and causes permafrost existence in the lower part of talus slopes and warmer sites in the upper part of the talus (Delaloye and Lambiel, 2005).

Even in relatively homogenous terrain BTS data and modelling results are not indicating always similar permafrost probability, but mismatches are very often in proximate neighbourhood and it seems that this is partly a problem of the map data resolution (Fig. 11).

A comparison of our permafrost distribution map of the Hohe Tauern region with the alpine wide permafrost map produced by the Interreg project PermaNet shows also some interesting features (Mair et al., 2011; Boeckli et al., 2012). The PermaNet model has a somewhat lower resolution (30 m DEM) and uses a threefold qualitative permafrost key with permafrost in
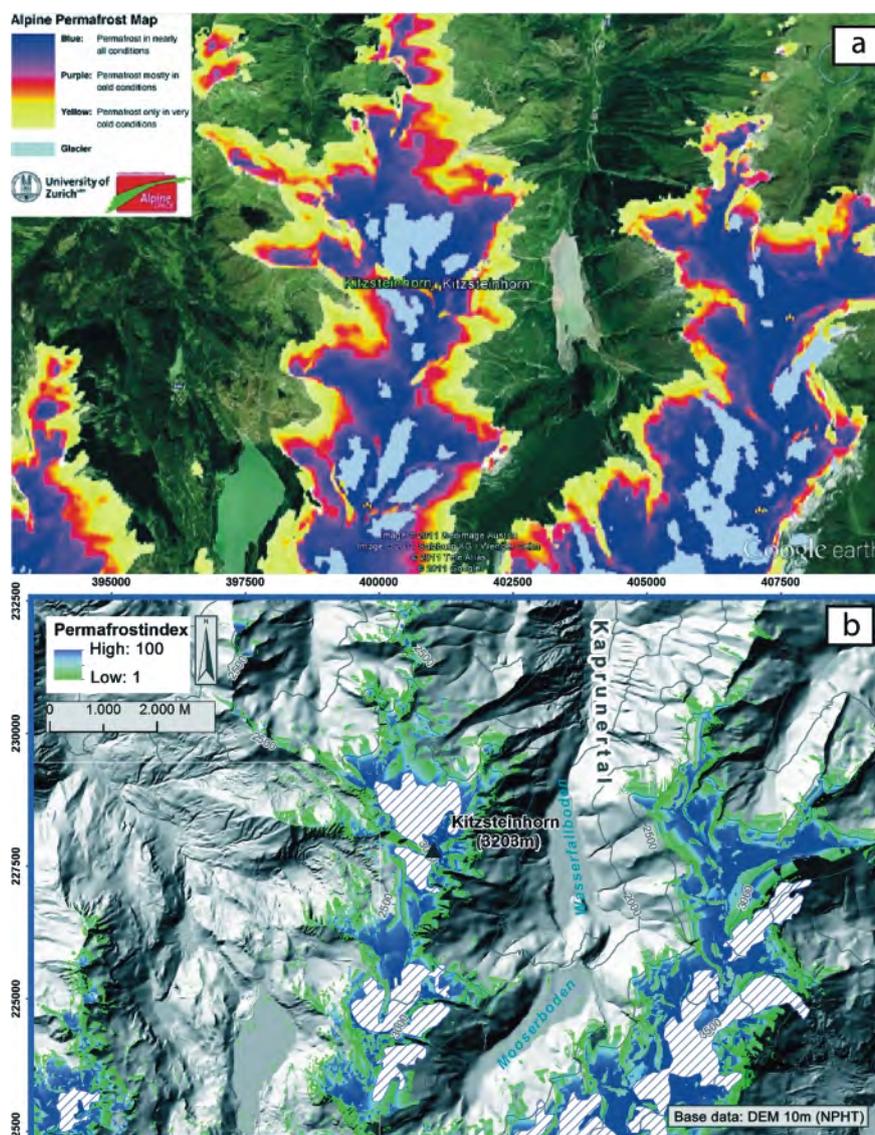

Figure 12: Comparison of permafrost probability maps for the testsite Kitzsteinhorn. (a) permafrost distribution map based on the modelling approach of PermaNet (Mair et al. 2011, Boeckli et al. 2012). (b) permafrost distribution map based on PERMAKART 3.0 used in this paper.

nearly all conditions, permafrost mostly in cold conditions, and permafrost only in very cold conditions. The approach is based on two statistical sub-models using a debris model and a rock model which are calibrated with rock glacier inventories and rock surface temperatures from the Alps (Boeckli et al., 2012). In Figure 12 both model outcomes for a typical region in the eastern Alps are presented. It seems that for regional purposes our new PERMAKART 3.0 model visualizes the permafrost pattern and isolated patches in a better and more realistic way. In contrast, the alpine wide PermaNet map is explicitly made for larger scales, but overestimates the permafrost presence in this part of the Eastern Alps. It is, however, a very useful approach and makes comparisons with other similar large scale mountain systems possible.

5.1 Potential scenarios

Knowledge concerning the present state and future develop-

ment of permafrost distribution is a research priority (Haeberli et al., 2010). In the European Alps climate change with warming trends can be observed since the second half of the 19th century and the mean annual air temperature increased in Austria since 1850 about 2°C (Böhm, 2009). The most visible indicator of change in the cryosphere is the strong retreat and loss of volume of alpine glaciers which relatively short reaction times. Mountain permafrost reacts also sensitively to warming but somewhat delayed and almost invisible. Borehole temperature measurements in mountain permafrost in the Alps controlled by the Swiss Permafrost Monitoring Network (PERMOS) provide valuable information about permafrost evolution (Nötzli and Vonder Mühll, 2010). As a near surface effect permafrost thawing may cause increased rock fall and debris flow activity (Deline et al., 2012; Gruber et al., 2004; Ravanel et al., 2010). Thawing and degradation of mountain permafrost within rock walls is considered to be an important process influencing the slope stability of steep slopes and rock faces in alpine mountain ranges. Krautblatter and Funk (2010) reported changes in rock mechanical properties of ice-filled rock clefts which may induce instability of larger portions of thawing rock permafrost. The interpretation of differing observations concerning permafrost thawing and degradation and potential natural hazards (e.g. rock falls, debris flows) remains a major challenge (Sattler et al., 2011; Haeberli et al., 2010). Efficient risk analysis and risk adaptation strategies largely depend on process understanding of permafrost-related evolution and hazards. Permafrost degradation is one potential effect of warming trends in the Alps. An important prerequisite for scenarios of permafrost development is an accurate mapping of the recent permafrost distribution. In a first attempt we calculated potential altitudinal shifts of lower limits of permafrost assuming rising mean annual temperatures of 1 and 2K, respectively. Based on the average lapse rate of -0.51°K/100m we estimate theoretical shifts of lower limits of permafrost of 195 and 390 m, respectively. According to our assumption an increase of only 1 or 2 K of mean annual ground temperature will lead to a potential reduction of permafrost areas of 70 and 90%, respectively. We are aware of the
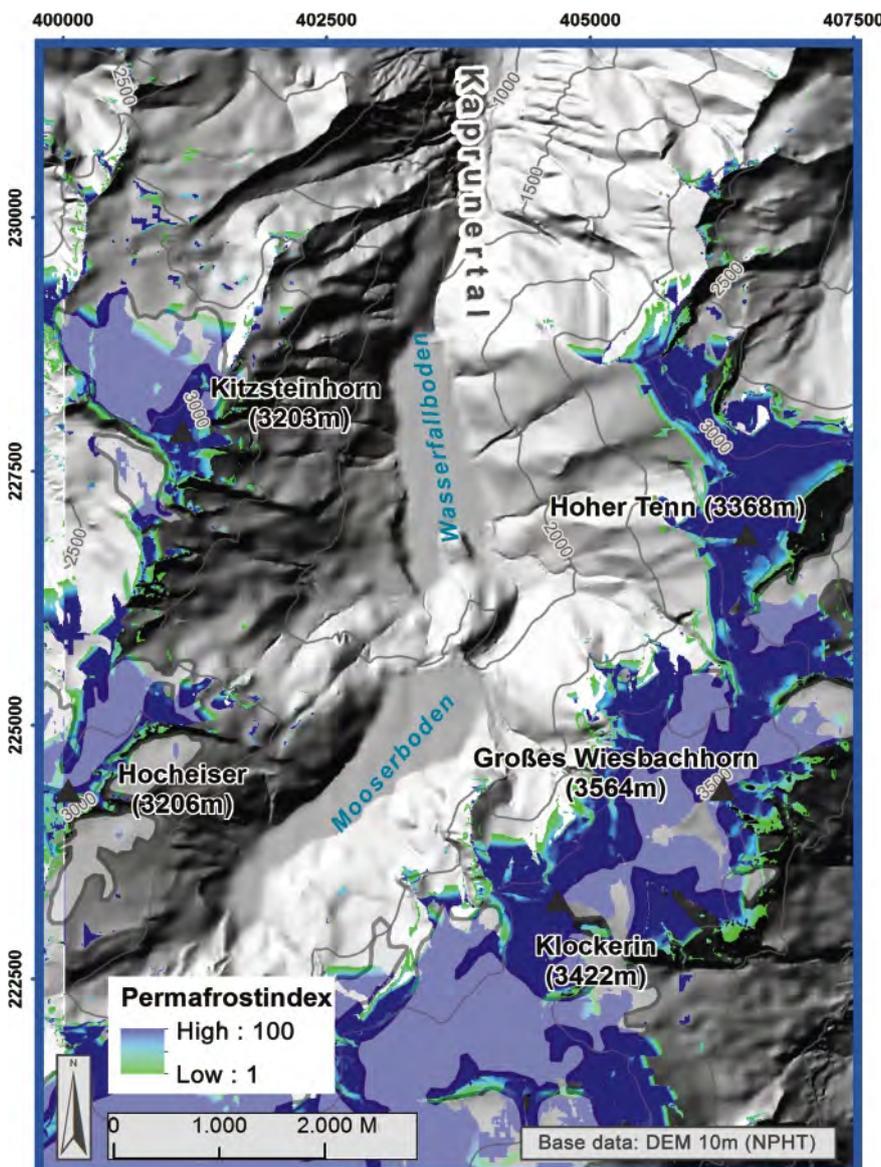

Figure 13: Scenario of potential permafrost distribution at the test site Kitzsteinhorn assuming a warming of 1K.

fact that this hypothetical assumption is a strong simplification due to non-existing linear relationships between air and ground temperature. Nevertheless the proposed simple scenario can be considered as a raw indicator how permafrost distribution may change if degradation will occur extensively (Fig. 13).

6. Conclusion and perspectives

For the first time a detailed permafrost distribution map is available for the region of the Hohe Tauern including the entire national park. Present permafrost occurrence is still a widespread phenomenon comprising 550 km² or approximately 13 % of the entire area. The produced permafrost map (resolution of 10 m) provides the basis for a deeper understanding of permafrost related hazards and assists decision-makers (e.g. engineers, planers, tourist guides) with relevant recommendations. For example, effective adaptation measures of engineering structures in mountain permafrost terrain and estimates about permafrost evolution depend on detailed knowledge concerning permafrost distribution.

As a rule of thumb, permafrost can be expected above 2500 m a.s.l. in northerly exposed slopes and above 3000 m a.s.l. in southerly exposed slopes (Fig. 6). The empirical PERMA-KART 3.0 model uses a total of 24 relief classes – eight different aspects and three different slope characteristics (including rock walls, steep slopes and slope-foot positions) and is performed with a new topoclimatic key and a transient probability index. The model was calibrated with additional data using field geophysics (DC-resistivity, GPR) and validated with more than 600 BTS data collected in six test areas. The validation shows that the model reflects reasonably well the permafrost occurrence at a regional level.

A major challenge remains the estimation of the future development of permafrost in the Alps. Strong topographic variations (e.g. snow cover and duration, subsurface structure, rock vs. debris area) and different permafrost temperatures cause a different sensitivity to climate change even at a local scale (Gruber and Haeberli, 2007). In a simple scenario assuming a temperature increase of 1 and 2 K we calculated a permafrost shift of 195 and 390, respectively. This scenario would result in potential permafrost degradation (surface area) of 70 and 90%, respectively.

Extensive borehole measurements in the Alps indicate the strong influence of snow cover on subsurface temperatures which enhance the heterogeneous pattern of permafrost in mountain areas (Noetzli and Vonder Mühll, 2010). A potential future application of the new PERMAKART 3.0 model is the integration of the cooling influence of a relatively thin (max. 40 cm) snow cover in early winter. This requires high resolution data on snow cover and duration.

References

Barsch, D., 1973. Refraktionsseismische Bestimmung der Obergrenze des gefrorenen Schuttkörpers in verschiedenen Blockgletschern Graubündens, Schweizer Alpen. Zeitschrift für Gletscherkunde und Glazialgeologie 9, 143-167.

Barsch, D., 1996. Rockglaciers: indicators for the present and former geoecology in high mountain environments. Springer-Verlag, Berlin.

Berthling, I. and Melvold, K., 2008. Ground penetrating radar. In: Hauck, C. and Kneisel, C. (eds.), Applied Geophysics in Periglacial Environments. Cambridge, Cambridge University Press. pp. 81-98.

Boeckli, L., Brenning, A., Gruber, A. and Noetzli, J., 2012. A statistical approach to modelling permafrost distribution in the European Alps or similar mountain ranges. The Cryosphere, 6, 125-140.

Böhm, R., 2009. Geändertes Umfeld durch Klimawandel? - Modified environment due to climate change? Wildbach- und Lawinenverbau 163, 34-50.

Bonnaventure, P.P. and Lewkowicz, A. G., 2008. Mountain permafrost probability mapping using the BTS method in two climatically dissimilar locations, northwest Canada. Canadian Journal of Earth Sciences, 45(4), 443-455.

Bonnanventure, P.P., Lewkowicz, A. G., Kremer, M. and Sawada, M.C., 2012. A permafrost probability model for southern Yukon and northern British Columbia, Canada. Permafrost and Periglacial Processes, 23 (1), 52-68.

Cremonese, E., Gruber, S., Phillips, M., Pogliotti, P., Boeckli, L., Noetzli, J., Suter, C., Bodin, X., Crepaz, A., Kellerer-Pirklbauer, A., Lang, K., Letey, S., Mair, V., Morra di Cella, U., Ravanel, L., Scapozza, C., Seppi, R. and Zischg, A., 2011. Brief Communication: „An inventory of permafrost evidence for the European Alps". The Cryosphere, 5, 651-657.

Delaloye, R. and Lambiel, C., 2005. Evidence of winter ascending air circulation throughout talus slope and rock glaciers situated in the lower belt of alpine discontinuous permafrost, Swiss Alps. Norsk Geografisk Tidsskrift - Norwegian Journal of Geography, 59(2), 194-203.

Deline, P., Gradent, M., Magnin, F., and Ravanel, L., 2012. The Morphodynamics of the Mont Blanc Massif in a changing cryosphere: a comprehensive review. Geografiska Annaler: Series A, Physical Geography, 94 (2), 265-283.

Ebohon, B. and Schrott, L., 2008. Modelling mountain permafrost distribution: A new permafrost map of Austria, In: D.L. Kane and K.M. Hinkel (eds.), Proceedings of the 9th International Conference on Permafrost, Fairbanks, Alaska, USA, 30 June - 03 July, pp. 397-402.

Etzelmüller, B., Berthling, I. and Sollid, J.L., 1998. The distribution of permafrost in Southern Norway; a GIS approach. In: A.G. Lewkowicz and M. Allard (eds.), Proceedings of the 7th International Conference on Permafrost, Nordicana, Yellowknife, Canada, 23-27 June, pp. 251-257.

Finsterwalder, S., 1928. Begleitworte zur Karte des Gepatschferners. Zeitschrift für Gletscherkunde, 16, 20-41.

Gruber, S., 2012. Derivation and analysis of a high-resolution estimate of global permafrost zonation. The Cryosphere, 6, 221–233.

Gruber, S. and Haeberli, W., 2007. Permafrost in steep bedrock slopes and its temperature-related destabilization following climate change. Journal of Geophysical Research, 112, F02S18, doi:10.1029/2006JF000547.

Gruber, S., Hoelzle, M. and Haeberli, W., 2004. Rock wall temperatures in the Alps: Modelling their topographic distribution and regional differences. Permafrost and Periglacial Processes, 15, 299-307.

Haeberli, W., 1973. Die Basis-Temperatur der winterlichen Schneedecke als möglicher Indikator für die Verbreitung von Permafrost in den Alpen. Zeitschrift für Gletscherkunde und Glazialgeologie, 9(1-2), 221-227.

Haeberli, W., 1975. Untersuchungen zur Verbreitung von Permafrost zwischen Flüelapass und Piz Grialetsch (Graubünden). Mitteilungen der Versuchsanstalt für Wasserbau, Hydrologie und Glaziologie der ETH Zürich, 17, 221 pp.

Haeberli, W., Noetzli, J., Arenson, L., Delaloye, R., Gaertner-Roer, I., Gruber, S., Isaksen, K., Kneisel, C., Krautblatter, M. and Phillips, M., 2010. Permafrost on mountain slopes - development and challenges of a young research field. Journal of Glaciology, 56(200), 1043-1058.

Harris, C., Vonder Mühll, D., Isaksen, K., Haeberli, W., Sollid, J.L., King, L., Holmlund, P., Dramis, F., Guglielmin, M. and Palacios, D., 2003. Warming permafrost in European mountains. Global and Planetary Change, 39(3-4), 215-225.

Hauck, C. and Kneisel, C., 2008. Applied geophysics in periglacial environments. Cambridge University Press, Cambridge, 256 pp.

Heggem, E.S.F., Juliussen, H. and Etzelmüller, B., 2005. The permafrost distribution in central-eastern Norway. Norsk Geografisk Tidsskrift, 59(2), 94-108.

Hoelzle, M., 1992. Permafrost occurrence from BTS measurements and climatic parameters in the Eastern Swiss Alps. Permafrost and Periglacial Processes, 3, 143-147.

Imhof, M., 1996. Modelling and verification of the permafrost distribution in the Bernese Alps (Western Switzerland). Permafrost and Periglacial Processes, 7, 267-280.

Isaksen, K., Hauck, C., Gudevang, E., Ødegård, R.S. and Sollid, J.L., 2002. Mountain permafrost distribution on Dovrefjell and Jotunheimen, southern Norway, based on BTS and DC resistivity tomography data. Norsk Geografisk Tidsskrift, 56(2), 122-136.

Janke, J.R. Williams, M.W. and Evans Jr., A., 2011. A comparison of permafrost prediction models along a section of Trail Ridge Road, Rocky Mountain National Park, Colorado, USA. Geomorphology, 138, 111-120.

Keller, F., 1992. Automated mapping of mountain permafrost using the program PERMAKART within the geographical information system ARC/INFO. Permafrost and Periglacial Processes, 3(2), 133-138.

Keller, F., Frauenfelder, R., Gardaz, J.M., Hoelzle, M., Kneisel, C., Lugon, R., Phillips, M., Reynard, E. and Wenkler, L., 1998. Permafrost map of Switzerland. Proceedings of the 7th International Conference on Permafrost, Yellowknife, Canada, pp. 557-562.

Kellerer-Pirklbauer, A., 2005. Alpine permafrost occurrence at its spatial limits: First results from the eastern margin of the European Alps, Austria. Norsk Geografisk Tidsskrift - Norwegian Journal of Geography, Oslo, 59, 184-193.

Keuschnig M., Hartmeyer I., Otto J.C. and Schrott L., 2011. A new permafrost and mass movement monitoring test site in the Eastern Alps – Concept and first results of the MOREXPERT project. Managing Alpine Future II - Inspire and drive sustainable mountain regions. Proceedings of the Innsbruck Conference, November 21-23, 2011, pp. 163-173.

Kneisel, C. and Kääb, A., 2007. Mountain permafrost dynamics within a recently exposed glacier forefield inferred by a combined geomorphological, geophysical and photogrammetrical approach. Earth Surface Processes and Landforms, 32, 1797-1810.

Krainer, K., 2007. Permafrost und Naturgefahren in Österreich. Ländlicher Raum, Bundesministerium für Land- und Forstwirtschaft, Umwelt und Wasserwirtschaft, Jahrgang 2007, 1-18.

Krainer, K. and Mostler, W., 2002. Hydrology of active rock glaciers: Examples from the Austrian Alps. Arctic, Antarctic and Alpine Research, 34, 142-149.

Krainer, K., Mostler, W. and Spötl, C., 2007. Discharge from active rock glaciers, Austrian Alps: a stable isotope approach. Austrian Journal of Earth Sciences, 100, 102-112.

Krautblatter, M. and Funk, D., 2010. A Rock/Ice mechanical model for the destabilisation of permafrost rocks and first laboratory evidence for the "reduced friction hypothesis". Proceedings of the 3rd European Conference on Permafrost, Svalbard, Spitsbergen, Norway, 13-17 June, p. 205.

Lewkowicz, A.G. and Bonnaventure, P.P., 2008. Interchangeability of mountain permafrost probability models, Northwest Canada. Permafrost and Periglacial Processes, 19, 49-62.

Lewkowicz, A.G., Bonnaventure, P.P., Smith, S.L. and Kuntz, Z., 2012. Spatial and thermal characteristics of mountain permafrost, northwest Canada. Geografiska Annaler: Series A, Physical Geography, 94 (2), 195-213.

Li, J., Sheng, Y., Wu, J., Chen, J. and Zhang, X., 2008. Probability distribution of permafrost along a transportation corridor in the north-eastern Qinghai province of China. Cold Regions Science and Technology, 59, 12-18.

Lieb, G.K., 1996. Permafrost und Blockgletscher in den östlichen österreichischen Alpen. In: Beiträge zur Permafrostforschung in Österreich. Arbeiten aus dem Institut für Geographie der Universität Graz, 33, 9-125.

Lieb, G.K., 1998. High-mountain permafrost in the Austrian Alps (Europe). In: A.G. Lewkowicz and M. Allard (eds.), Proceedings of the 7th International Conference on Permafrost, Nordicana, Yellowknife, Canada, 23-27 June, pp. 663-668.

Mair, V., Zischg, A., Lang, K., Tonidandel, D., Krainer, K., Kellerer-Pirklbauer, A., Deline, P., Schoeneich, P., Cremonese, E., Pogliotti, P., Gruber, S., Böckli, L., 2011. PermaNET - Permafrost Long-term Monitoring Network. Synthesis report, INTERPRAEVENT Schriftenreihe 1, Report 3. Klagenfurt.

Noetzli, J. and Gruber, S., 2009. Transient thermal effects in Alpine permafrost. The Cryosphere, 3, 85-99.

Noetzli, J. and Vonder Mühll, D. (eds.), 2010. PERMOS 2010. Permafrost in Switzerland 2006/2007 and 2007/2008. Glaciological Report (Permafrost) No. 8/9 of the Cryospheric Commission (CC) of the Swiss Academy of Sciences (SCNAT), 68 pp.

Noetzli, J., Gruber, S., Kohl, T., Salzmann, N. and Haeberli, W., 2007. Three-dimensional distribution and evolution of permafrost temperatures in idealized high-mountain topography. Journal of Geophysical Research-Earth Surface, 112(F2), F02S13, doi:10.1029/2006JF000545.

Otto, J.C. and Sass, O., 2006. Comparing geophysical methods for talus slope investigations in the Turtmann valley (Swiss Alps). Geomorphology, 76(3-4), 257-272.

Otto, J.-C., Kogler, P. , Ebohon, B. and Schrott, L., 2009. Geophysikalische Untersuchung eines Moränendammes im oberen Amertal, Land Salzburg. Abschlussbericht ÖBB (unpublished).

Otto, J-C., Keuschnig, M., Götz, J., Marbach, M. and Schrott, L., 2012. Detection of mountain permafrost by combining high-resolution surface and subsurface information - An example from the Glatzbach catchment, Austrian Alps. Geografiska Annaler: Series A, Physical Geography, 94 (1), 43-57.

Patzelt, G. and Haeberli, W., 1982. Permafrostkartierung im Gebiet der Hochebenkar-Blockgletscher, Obergurgl, Ötztaler Alpen. Zeitschrift für Gletscherkunde und Glazialgeologie, Innsbruck, 18(2), 127-150.

Ravanel, L., Allignol, P., Deline, P., Gruber, S. and Ravello, M., 2010. Rock falls in the Mont Blanc Massif in 2007 and 2008. Landslides, 7(4), 493-501.

Ridefelt, H., Etzelmuller, B., Boelhouwers, J. and Jonasson, C., 2008. Mountain permafrost distribution in the Abisko region, sub-Arctic northern Sweden. Norwegian Journal of Geography, 67, 276-289.

Sattler, K., Keiler, M., Zischg, A. and Schrott, L., 2011. On the connection between debris flow activity and permafrost degradation: A case study from the Schnalstal, South Tyrolean Alps, Italy. Permafrost and Periglacial Processes, 22, 254-265.

Schrott, L., 1994. Die Solarstrahlung als steuernder Faktor im Geosystem der subtropischen semiariden Hochanden, Agua Negra, San Juan, Argentinien. Heidelberger Geographische Arbeiten, 94, 199 pp.

Schrott, L., 1996. High mountain permafrost and its relation to landform and solar radiation. A case study in the High Andes of San Juan, Argentina. In: M. Panizza, M. Soldati, D. Barani and M. Bertacchini (eds.), The Erasmus 94-95 Programme in Geomorphology, Intensive Course Tyrol (Austria) and Student Mobility. Dipartimento di Scienze della Terra, Università degli Studi di Modena, 77-87.

Schrott, L. and Sass, O., 2008. Application of field geophysics in geomorphology: advances and limitations exemplified by case studies. Geomorphology, 93, 55-73.

Tanarro, L.M., Hoelzle, M., García, A., Ramos, M., Gruber, S., Gómez, A., Piquer, M. and Palacios, D., 2001. Permafrost distribution modelling in the mountains of the Mediterranean. Corral del Veleta, Sierra Nevada, Spain. Norsk Geografisk Tidsskrift Norwegian Journal of Geography, 55, 253-260.

Trabant, P. K., 1988. Applied High-Resolution Geophysical Methods, Upper Saddle River, Prentice Hall, 279 pp.

Lothar SCHROTT[1)*], Jan-Christoph OTTO[1)], Felix KELLER[2)]

[1)] University of Salzburg, Department of Geography and Geology, Salzburg, Austria;

[2)] Academia Engiadina, Samedan, Schwitzerland;

[*)] Corresponding author, lothar.schrott@sbg.ac.at